

Provided for non-commercial research and education use.  
Not for reproduction, distribution or commercial use.



This article appeared in a journal published by Elsevier. The attached copy is furnished to the author for internal non-commercial research and education use, including for instruction at the authors institution and sharing with colleagues.

Other uses, including reproduction and distribution, or selling or licensing copies, or posting to personal, institutional or third party websites are prohibited.

In most cases authors are permitted to post their version of the article (e.g. in Word or Tex form) to their personal website or institutional repository. Authors requiring further information regarding Elsevier's archiving and manuscript policies are encouraged to visit:

<http://www.elsevier.com/copyright>



Contents lists available at ScienceDirect

European Polymer Journal

journal homepage: [www.elsevier.com/locate/europolj](http://www.elsevier.com/locate/europolj)

# Preparation and characterization of single-hole macroporous organogel particles of high toughness and superfast responsivity

Deniz C. Tuncaboğlu, Oguz Okay\*

Department of Chemistry, Istanbul Technical University, 34469 Maslak, Istanbul, Turkey

## ARTICLE INFO

### Article history:

Received 30 January 2009

Received in revised form 14 March 2009

Accepted 1 April 2009

Available online 7 April 2009

### Keywords:

Organogel beads

Macroporous particles

Butyl rubber

Cryogelation

Elasticity

Swelling

## ABSTRACT

Crosslinked macroporous polymer particles containing a single large hole in their surfaces were prepared by solution crosslinking of butyl rubber (PIB) in benzene using sulfur monochloride ( $S_2Cl_2$ ) as a crosslinking agent. The reactions were carried out within the droplets of frozen solutions of PIB and  $S_2Cl_2$  at  $-18\text{ }^\circ\text{C}$ . Spherical millimeter-sized organogel beads with a polydispersity of less than 10% were obtained. The particles display a two phase morphology indicating that both cryogelation and reaction-induced phase separation mechanisms are operative during the formation of the porous structures. The beads exhibit moduli of elasticity of 1–4 kPa, much larger than the moduli of conventional nonporous organogel beads formed at  $20\text{ }^\circ\text{C}$ . The gel particles also exhibit fast responsivity against the external stimulus (solvent change) due to their large pore volumes (4–7 ml/g). The gel beads prepared at  $-18\text{ }^\circ\text{C}$  are very tough and can be compressed up to about 100% strain during which almost all the solvent content of the particles is released without any crack development. The sorption–squeezing cycles of the beads show that they can be used in separation processes in which the separated compounds can easily be recovered by compression of the beads under a piston.

© 2009 Elsevier Ltd. All rights reserved.

## 1. Introduction

Porous particles have a wide range of applications in various areas such as tissue engineering, catalysis, chromatography, and separation. Hollow polymer particles or microcapsules are also of technological importance in controlled release of drugs, cosmetics, or in the removal of pollutants [1–5]. Such particles are commonly prepared by coating the surface of template particles with a thin layer of desired material, followed by removal of the core particles using chemical etching [4]. Other methods to generate hollow structures include emulsion droplets, self-assembly, phase separation, and polymer micelles [6–8]. However, since the diffusion through the closed shell of the particles is a slow process, hollow polymer particles with porous shells, or, with a single-hole in their surfaces are particular interest because they can readily upload drugs

or reagents [9–11]. Im et al. showed that polystyrene hollow particles with controllable holes in their surfaces can be prepared by means of low temperature swelling of polymer particles [9,10]. Recently, Guan et al. demonstrated formation of such particles by polymerization – crosslinking reactions at the surface of carboxyl-capping polystyrene colloids [12]. He et al. prepared hollow polymer particles with porous shells by self-assembling of sulfonated polystyrene latex particles at the interface of emulsion droplets [13].

Herein, we introduce a simple strategy that allows the preparation of millimeter-sized macroporous organogel particles containing a single large hole in their surfaces. The starting material of the particles is a linear polyisobutylene containing small amounts of internal unsaturated groups (isoprene units), known as butyl rubber. Previous work within this department has shown that in dilute benzene solutions, butyl rubber can easily be crosslinked using sulfur monochloride ( $S_2Cl_2$ ) as a crosslinking agent at temperatures down to  $-18\text{ }^\circ\text{C}$ , i.e., about  $23\text{ }^\circ\text{C}$  below the

\* Corresponding author. Tel.: +90 212 2853156; fax: +90 212 2856386.  
E-mail address: [okay@itu.edu.tr](mailto:okay@itu.edu.tr) (O. Okay).

freezing point of the solution [14,15]. As first demonstrated by Lozinsky et al. in 1984 [16], the occurrence of the crosslinking reactions below the freezing point of organic solutions is due to the presence of unfrozen regions in the apparently frozen reaction system [17]. It was shown that, when a 5% butyl rubber solution is frozen at  $-18\text{ }^{\circ}\text{C}$ , 14% of benzene remains unfrozen in the apparently frozen system [14]. Thus, as benzene freezes, the polymer chains are excluded from the benzene crystals and, they accumulate in the unfrozen microregions, making the butyl rubber concentration in these regions about 36%, high enough to conduct the crosslinking reactions even at  $-18\text{ }^{\circ}\text{C}$ . After the crosslinking reactions in the unfrozen zones and, after melting of benzene crystals, a macroporous material was produced whose microstructure is a negative replica of the crystals formed [14].

Our strategy to prepare single-hole macroporous gel particles is to conduct the crosslinking reactions within the droplets of frozen solutions of butyl rubber at  $-18\text{ }^{\circ}\text{C}$ . The crosslinking reactions occurring in the unfrozen zones of the apparently frozen droplets lead to the formation of spherical, monodisperse single-hole porous particles of high toughness and superfast responsivity. Here, we also show that these particles can be used in separation processes in which the separated compounds or pollutants can easily be recovered by compression of the beads under a piston. The reusability of the gel beads and the recoverability of the pollutants were demonstrated by conducting successive sorption–squeezing cycles of the beads in contact with toluene and crude oil.

## 2. Experimental

### 2.1. Materials

Butyl rubber 365 (PIB, Exxon Mobil) with an unsaturation degree of 2.3 mol% and a Mooney viscosity of 33 was used in the gelation experiments. It was dissolved in toluene following by precipitation into methanol and drying at room temperature under vacuum to constant mass. Sulfur monochloride (Riedel de Haen) was used as received. Ethylene glycol (Fluka and Merck), arabic gum (technical grade), sodium dodecyl sulfate (Sigma–Aldrich), ethanol (Riedel de Haen), and sodium chloride (NaCl, Riedel de Haen) were also used as received. Crude oil, which was used in the sorption experiments, was provided from Ozan Sungurlu wells, Turkey ( $d = 0.89\text{ g/ml}$ , viscosity = 350 cP at  $25\text{ }^{\circ}\text{C}$ ).

### 2.2. Preparation of conventional PIB particles

We first conducted the crosslinking reactions at  $20\text{ }^{\circ}\text{C}$  to obtain nonporous PIB beads as a reference material. Spherical PIB beads of diameters between 0.7 and 5 mm were obtained by suspension crosslinking of the organic solutions of PIB and the crosslinking agent  $\text{S}_2\text{Cl}_2$  in ethylene glycol (continuous phase) containing arabic gum (0.5%), sodium dodecyl sulfate (0.1%) and NaCl (0.3%) as the stabilizer system. Following parameters were fixed in our experiments:

Volume ratio of continuous/organic phase: 10/1.  
PIB concentration in the organic phase: 10 w/v%.  
Reaction time: 17 h.

In a typical experiment, 100 ml of ethylene glycol containing arabic gum (0.5 g), sodium dodecyl sulfate (0.1 g) and NaCl (0.3 g) were first introduced into a 150-ml glass jar and stirred for about 1 h. Separately, butyl rubber (1 g) dissolved in 10 ml of benzene was mixed with the crosslinking agent sulfur monochloride in an Erlenmeyer flask. The organic phase was then transferred into the continuous phase and the reaction was allowed to proceed for 17 h at  $20 \pm 1\text{ }^{\circ}\text{C}$ . After the reaction, the beads were separated from the continuous phase and they were washed several times with water and then with toluene. The average size of the beads swollen in toluene could be regulated between 2 and 7 mm by the amounts of the stabilizers and the crosslinker  $\text{S}_2\text{Cl}_2$  as well as by the stirring rate during reactions. The polydispersity PD, i.e., the relative standard deviation of the beads was large and ranged between 20% and 60%.

### 2.3. Preparation of single-hole macroporous PIB particles

Solution crosslinking of butyl rubber (PIB) was carried out in benzene using  $\text{S}_2\text{Cl}_2$  as a crosslinking agent. The polymer concentration was fixed at 10 w/v% while the  $\text{S}_2\text{Cl}_2$  concentration was varied.  $\text{S}_2\text{Cl}_2$  content of the reaction solution,  $\text{S}_2\text{Cl}_2\%$ , was expressed as the volume of  $\text{S}_2\text{Cl}_2$  added per 100 g of PIB. Since PIB contains 2.3 mol% isoprene units, the molar masses of isobutylene, isoprene units, and  $\text{S}_2\text{Cl}_2$  are 56, 68, and 135 g/mol, respectively, and the density of  $\text{S}_2\text{Cl}_2$  is 1.68 g/ml, a multiplication factor of 0.30 converts  $\text{S}_2\text{Cl}_2\%$  into the moles of crosslinking agent added per mole of isoprene unit in the polymer. Porous particles were obtained by conducting the crosslinking reactions at  $-18\text{ }^{\circ}\text{C}$ . Two techniques were used:

Technique A: 10 ml of benzene containing PIB (1 g) and the crosslinking agent  $\text{S}_2\text{Cl}_2$  was added dropwise into excess liquid nitrogen to create small frozen organic droplets. As each droplet touches the liquid nitrogen, nitrogen starts to boil while the droplet spins on the liquid surface until it falls down into the liquid nitrogen. After complete addition of the organic phase, the frozen droplets were transferred into an excess of ethanol at  $-18\text{ }^{\circ}\text{C}$  as the continuous phase and the crosslinking reactions were carried out for 17 h.

Technique B: 10 ml of benzene containing PIB (1 g) and the crosslinking agent  $\text{S}_2\text{Cl}_2$  was added dropwise into a continuous phase consisting of ethylene glycol and ethanol in a volume ratio of 1:4 and at a temperature of  $-18\text{ }^{\circ}\text{C}$ . The temperature of the continuous phase was controlled using a thermostated bath filled with ethanol (Huber CC1, Germany). Since the density of the continuous phase is close to that of the organic phase, the droplets slowly fall down the solution (falling distance = 4.5 cm), during which they start to freeze so that the coalescence of the particles could be prevented. After complete addition of the organic phase, the reactions were conducted for 17 h at  $-18\text{ }^{\circ}\text{C}$  and then, the particles were separated as described above.

## 2.4. Swelling measurements

Swelling measurements were conducted on individual gel beads equilibrium swollen in toluene. The beads were placed separately in glass vials containing an excess of toluene at  $21 \pm 0.5$  °C. In order to reach swelling equilibrium, the beads were immersed in toluene for at least 2 weeks replacing the toluene many times. The swelling equilibrium was tested by monitoring the diameter of the gel beads using an image analyzing system consisting of a microscope (XSZ single Zoom microscope), a CDD digital camera (TK 1381 EG) and a PC with the data analyzing system Image-Pro Plus. The swelling equilibrium was also tested by weighing the gel beads. Thereafter, the gel beads equilibrium swollen in toluene were first added into methanol (poor solvent) and then dried in vacuum at room temperature. The equilibrium volume and the equilibrium weight swelling ratios of the beads,  $q_v$  and  $q_w$ , respectively, were calculated as:

$$q_v = (D/D_{dry})^3 \quad (1)$$

$$q_w = m/m_{dry} \quad (2)$$

where  $D$  and  $D_{dry}$  are the diameters of the equilibrium swollen and dry beads, respectively,  $m$  and  $m_{dry}$  are the weights of beads after equilibrium swelling in toluene and after drying, respectively. Note that the swelling measurements were conducted on at least six individual beads prepared under the same experimental condition and the results were averaged.

For the measurement of the deswelling rates of gel beads, the equilibrium swollen gel beads in toluene were immersed in methanol at 21 °C. The volume changes of beads were measured in-situ by following the diameter of the samples under microscope using the image analyzing system. For the measurement of the swelling rates of beads, the collapsed gel beads in methanol were transferred into toluene at 21 °C. The diameter changes of the beads were also monitored as described above. The results were given as the relative volume swelling ratio  $V_{rel} = (D_t/D)^3$  where  $D_t$  is the gel diameter at time  $t$ .

## 2.5. Elasticity tests

Uniaxial compression measurements were performed on individual gel beads in their swollen states. All the mechanical measurements were conducted in a thermostated room of  $21 \pm 0.5$  °C. The stress–strain isotherms were measured by using an apparatus previously described [18–20]. Briefly, a gel bead of 3–13 mm in diameter was placed on a digital balance (Precisa 320 XB – 220A, readability and reproducibility = 0.1 mg). A load was transmitted vertically to the gel through a rod fitted with a PTFE end-plate. The force  $F$  acting on the gel was calculated from the reading of the balance  $m$  as  $F = m g$ , where  $g$  is the gravitational acceleration. The resulting deformation  $\Delta D$  was measured using a digital comparator (IDC type Digimatic Indicator 543-262, Mitutoyo Co.), which was sensitive to displacements of  $10^{-3}$  mm. The force and the resulting deformation were recorded after 20 s of relaxation. The

measurements were conducted up to about 20% compression.

We first conducted the compression measurements on individual gel beads immersed in a large excess of toluene. However, no reproducible results were obtained from these measurements, probably due to the motion of the bead during compression. Measurements conducted outside of the toluene phase gave reproducible results. The weight loss of single beads during the measurement due to solvent evaporation or due to the applied force was found to be negligible. This was achieved by keeping the measurement time as short as possible. One measurement took only less than 10 min involving 10–30 data points.

## 2.6. Texture determination and porosity of beads

For the texture determination of dried gel beads, scanning electron microscopy (SEM) studies were carried out at various magnifications between 50 and 2000 times (Jeol JSM 6335F Field Emission SEM). Prior to the measurements, network samples were sputter-coated with gold for 3 min using Sputter-coater S150 B Edwards instrument. The texture of the gel beads at various swelling states was investigated under XSZ single Zoom microscope using the image analyzing system Image-Pro Plus. For this purpose, the samples swollen in toluene were first immersed into liquid nitrogen for 1 min and then, they were cut into thin slices of about 1 mm in thickness. The measurements were conducted at room temperature and at magnifications between 10 and 100 times.

The pore volume  $V_p$  of the beads was estimated through uptake of methanol of the organogel beads. The gel beads swollen in toluene were transferred into methanol and methanol was refreshed several times until the mass of the beads remains unchanged. Since methanol is a nonsolvent for PIB [21], it only enters into the pores of the polymer networks. Thus,  $V_p$  (ml pores in one gram of dry polymer network) was calculated as

$$V_p = (m_M - m_{dry}) / (d_M m_{dry}) \quad (3)$$

where  $m_M$  is the weight of the bead immersed in methanol after 3 h and  $d_M$  is the density of methanol (0.792 g/ml).

## 3. Results and discussion

### 3.1. Formation of organogel particles

To obtain porous particles, the crosslinking reactions were carried out within the frozen organic droplets at  $-18$  °C. As mentioned in the experimental part, two techniques were used: according to the first technique (technique A), the organic solution containing PIB and the crosslinking agent  $S_2Cl_2$  was dropped into liquid nitrogen to create small frozen organic droplets at  $-196$  °C. Then, the frozen droplets were transferred into ethanol at  $-18$  °C as the continuous phase and the reactions were carried out for 17 h. Images shown at the first and second rows of Fig. 1 were taken from frozen solution droplets in liquid nitrogen, and from PIB beads just after preparation, respectively, at two different magnifications. The image

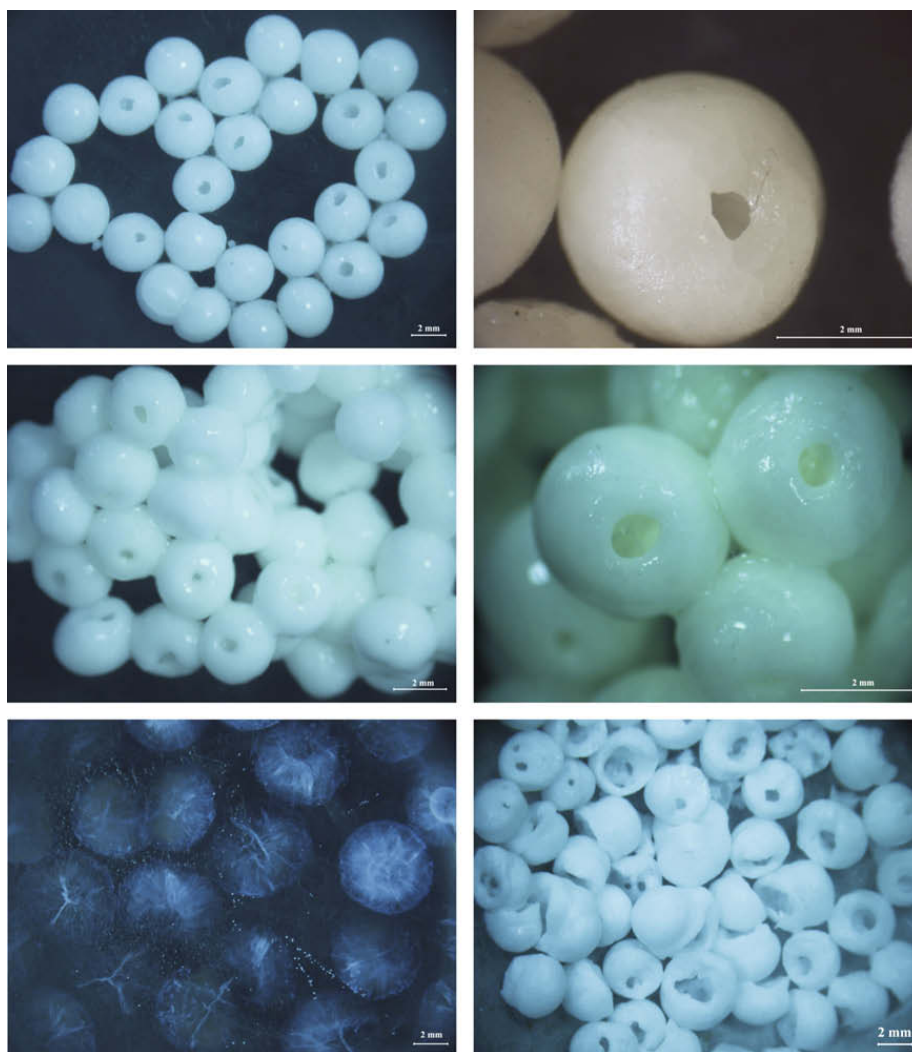


**Fig. 1.** Optical microscopy images of PIB beads formed by technique A. First row: Frozen PIB solution droplets in liquid nitrogen. Second row: PIB beads just after preparation. Third row, left: PIB beads equilibrium swollen in toluene.  $S_2Cl_2 = 20$  v/w %. PIB concentration = 10 w/v%. Third row, right: Droplets of frozen PIB solution in liquid nitrogen.  $S_2Cl_2 = 20$  v/w %. PIB concentration = 1 w/v %. All the scaling bars are 2 mm.

at the bottom-left of Fig. 1 was taken from the PIB beads after equilibrium swelling in toluene. It is seen that, freezing of PIB solution in liquid nitrogen results in the formation of uniform frozen solution droplets with an opening in their shells. The spherical shape and the morphology of the frozen droplets remained unchanged after the cross-linking reactions as well as after swelling of the crosslinked particles in toluene. Using this technique, we were able to obtain uniform and spherical millimeter-sized organogel beads with a polydispersity PD, i.e., a relative standard deviation of less than 6%. The diameter of the gel beads could be adjusted by changing the tip diameter ( $D_{tip}$ ) of the pipettes from which the organic solution was dropped into liquid nitrogen. For example, as  $D_{tip}$  is increased from 2.1 to 7.3 mm, diameter of the swollen particles in toluene increased from 4.9 to 6.7 mm while the diameter of the opening on the surface of the swollen particles remained at  $0.7 \pm 0.1$  mm. It should be noted that, by decreasing the PIB concentration of the organic solution, the size of the opening on the particle surfaces could be further increased. For example, bottom-right image of Fig. 1 shows

the frozen droplets in liquid nitrogen having a PIB concentration of 1%; the average diameter of the opening on the surface of frozen droplets is 3.8 mm. However, gelation reactions of the frozen droplets at such low concentration of PIB resulted in the formation of agglomerates. To characterize the shape and the size of the beads formed by technique A, swollen beads were cut into two halves and they were investigated by optical microscopy. As seen from Fig. 2, the hole starting from one of the poles of the swollen bead continuous up to the equator in the form of a cylinder.

The second technique for the preparation of porous particles (technique B) involves dropwise addition of the organic solution containing PIB and  $S_2Cl_2$  into a continuous phase at  $-18$  °C. We should note that, if the reactions were carried out under the condition of the usual suspension crosslinking technique, that is, under stirring of the continuous phase, odd-shaped gel particles with a broad size distribution were obtained, probably due to the collisions between the frozen droplets. Moreover, at low stirring rates, agglomerates of organogel particles were obtained.

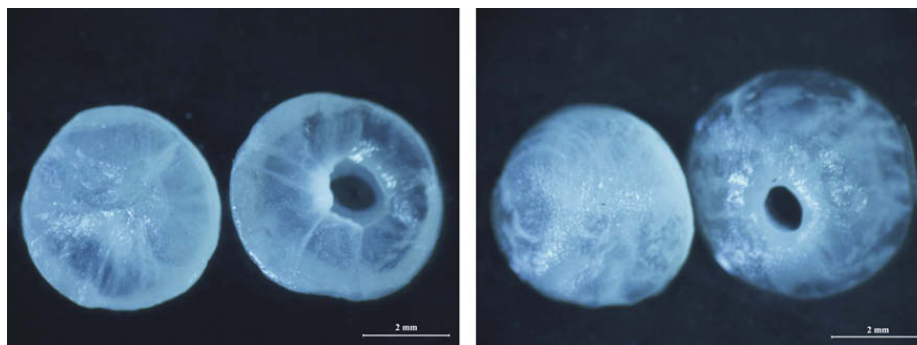


**Fig. 2.** Optical microscopy images of a swollen bead formed by technique A after cutting into two pieces. Views are from the equator to the pole (left) and from reverse direction (right).  $S_2Cl_2 = 20$  v/w%. PIB concentration = 10 w/v%. Scaling bars are 2 mm.

Therefore, no stirring was provided during the reactions and the density of the continuous phase was so adjusted that the droplets slowly fall down the solution. Use of an ethylene glycol–ethanol mixture (1:4 by volume) having a density close to that of the organic droplets was found to be ideal for the formation of PIB beads. In this way, uniform and spherical millimeter-sized beads with a PD of less than 10% were obtained. The optical images in Fig. 3 show the beads after preparation (A), and after equilibrium swelling in toluene (B) and in methanol (C). As by the first technique, PIB beads have openings on their surfaces and the openings became more visible by immersing the beads in a poor solvent such as methanol. The shape of the hole inside the beads was the same as that observed in beads formed by technique A (Fig. 2). Further, the size of the PIB beads formed by this technique could also be varied by changing the size of the droplets, i.e., by changing the diameter of the pipette tips.

### 3.2. Properties of the particles

Swelling, porosity, and elasticity characteristics of the beads prepared at  $-18$  °C with and without precooling in liquid nitrogen (techniques A and B, respectively) were collected in Table 1. All the measurements were conducted on individual gel beads and the results were averaged. The standard deviations are shown in the parenthesis. For comparison, the properties of conventional, nonporous PIB beads prepared using suspension crosslinking at 20 °C are also shown in Table 1. The organogel beads swell in tolu-

**Table 1**

Swelling, porosity, and elasticity characteristics of three types of PIB beads prepared at a PIB concentration of 10 w/v% in benzene. The conventional type beads were prepared at 20 °C while the others were prepared at  $-18$  °C with and without precooling in liquid nitrogen by techniques A and B, respectively.

Type	$S_2Cl_2$ (%)	$q_w$	$q_v$	$V_p/ml\ g^{-1}$	$G/kPa$
Technique A	10	38 (4)	29 (1)	5.6 (0.4)	–
Technique A	20	25 (1)	23 (2)	5.3 (0.7)	1.43 (0.40)
Technique B	5	(a)	(a)	(a)	0.64 (0.20)
Technique B	10	21 (1)	17 (1)	6.9 (0.2)	1.60 (0.30)
Technique B	20	17 (2)	14 (1)	4.2 (0.4)	3.60 (0.45)
Conventional	20	28 (2)	20 (2)	0.7 (0.1)	0.27 (0.08)

(a) These gel particles were too weak so that their shape disrupted during drying.

ene (good solvent) about 20–40 times their dry weights; decreasing  $S_2Cl_2\%$  increases their weight swelling ratios. Thus, although the concentration of the crosslinking agent  $S_2Cl_2$  used in the gel preparation was in a large excess, i.e., between 5% and 20% corresponding to 1.5–6 mol  $S_2Cl_2$  per mol of internal unsaturated group of PIB, the swelling ratio sensitively depends on  $S_2Cl_2$  concentration in the reaction solution. This is probably due to the cyclization reactions occurring between sulfur chloride and unsaturated groups on the same polymer chains. Indeed, previous studies showed that the critical amount of  $S_2Cl_2$  required for the onset of gelation during the solution crosslinking of PIB at 20 °C was 60-fold larger than the theoretical value [21]. The total volume of the pores in the beads was esti-

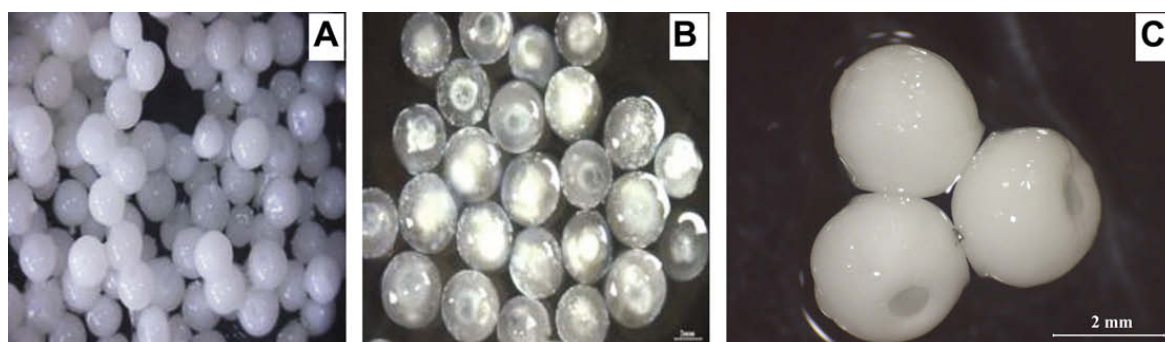


**Fig. 3.** Optical microscopy images of PIB beads formed by technique B after preparation (A), after equilibrium swelling in toluene (B) and in methanol (C). The scaling bars are 2 mm.  $S_2Cl_2 = 10$  v/w%. PIB concentration = 10 w/v%.

mated from the uptake of methanol (poor solvent). The gel beads prepared at  $-18\text{ }^{\circ}\text{C}$  exhibit pore volumes ( $V_p$ ) in the range of 4–7 ml/g compared to the negligible pore volume of the conventional beads. This is a consequence of the frozen zones inside the droplets at  $-18\text{ }^{\circ}\text{C}$  acting as templates during the reactions.

It should be mentioned that the porosity measurements were carried out before drying of the gel beads. Thus, toluene in the equilibrium swollen particles was replaced with methanol, which is a poor solvent for PIB so that it only fills the pores of the particles. However, if the porosity measurements were conducted starting from dry gel particles, that is, if dry particles were immersed into methanol, the pore volumes  $V_p$  found were much lower. For example, at  $\text{S}_2\text{Cl}_2$  concentration of 20%,  $V_p = 0.72 \pm 0.33\text{ ml/g}$  and  $0.80 \pm 0.36\text{ ml/g}$  for beads formed by techniques A and B, respectively, i.e., close to the value obtained for the nonporous beads (Table 1). The results suggest that the pore structure of the particles is not stable and collapse during their drying process. Another evidence for the porous collapse was obtained from the swelling measurements of beads starting from their dry states; the weight swelling ratio  $q_w$  was 3.4 g/g for dry beads formed by both technique, i.e., about 80% lower than the  $q_w$  of swollen beads (Table 1). Since the weight swelling represents the amount of the solvent locating in both pores and in the polymer region, this decrease also reflects the collapse of the porous structure of the particles.

The internal morphology of PIB beads was investigated at various swelling states using optical and scanning electron microscopy (SEM) methods. Fig. 4 shows optical and SEM images of the beads formed by technique A (upper panel) and B (bottom panel) at various swelling states. The swelling degree decreases from left to right and the far left images (C and D) were taken from dry beads by SEM. The size of the pores in swollen beads is in the range of  $10^0$ – $10^1\text{ }\mu\text{m}$ ,

while it decreases as the solvent is removed from the gels. The polymer matrix seems to collapse so that the pore structure partially disappears during the evaporation of the solvent. In the dry state, a regular structure consisting of pores of  $10^0\text{ }\mu\text{m}$  in diameter is seen from the SEM images. Another point seen in the bottom-right image of Fig. 4 is that the morphology of the center region of the bead significantly differs from that of the shell region. The center of the gel network consists of agglomerates of large polymer domains; the interstices between these domains constitute the porous structures. The structure of this region looks like cauliflower typical for porous gels obtained by reaction-induced phase separation technique [22]. In contrast, however, the shell regions consist of pores of  $10^0\text{ }\mu\text{m}$  in diameter separated by thick pore walls indicating that the particle exhibits a two phase morphology. Similar images were also obtained from the center region of the beads formed by technique A. The two phase morphology of the particles can also be seen from the images of swollen beads (bottom-left image in Figs. 1 and 3B), where the center regions are more opaque than the shell regions.

Formation of macroporous polymer particles with an unusual morphology can be explained according to the following scenario: During freezing of the solution droplets, the polymer chains and the crosslinker molecules are expelled from the benzene crystals and, they concentrate within the channels between the crystals. Moreover, benzene is a poor solvent for PIB with an upper critical solution temperature of  $24.5\text{ }^{\circ}\text{C}$  [23–25]. Thus, as the droplets are cooled, a liquid–liquid phase separation may also occur in their interior due to the  $\chi$ -induced syneresis [22]. The separated polymer-rich phase agglomerate into larger clusters and continuing the reactions increase the number of clusters in the system so that the polymer phase becomes continuous. Appearance of agglomerates of large polymer domains in regions close to the hole of the parti-

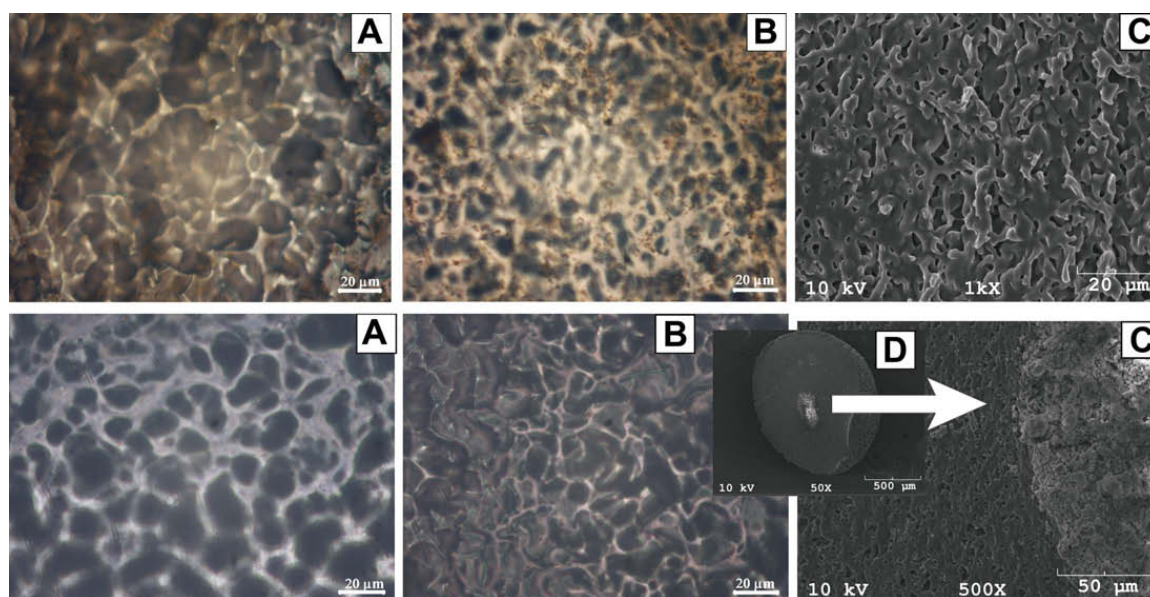


**Fig. 4.** Optical microscopy and SEM images of the beads formed by technique A (upper panel) and B (bottom panel) at various swelling states. The swelling degree of beads decreases from left to right and, the far left SEM images (C and D) were taken from dry beads. The bottom-right image (C) is a magnified version of the image (D).  $\text{S}_2\text{Cl}_2 = 20\text{ v/w}\%$ . PIB concentration = 10 w/v%.

cles indicates that the phase separation mechanism is operative in the inner part of the droplets. The crosslinking reactions in the polymer-rich unfrozen channels in the shell as well as in the phase separated domains in the interior lead to the formation of dense polymer domains surrounding the solid benzene crystals acting as templates. Thus, the porous structure of the particles forms by both cryogelation and reaction-induced phase separation mechanisms. Moreover, although the formation mechanism of a single large hole in the surface of the particle is unclear yet, polymer/solvent phase separation during freezing and subsequent interfacial free energy minimization, as suggested by Yin and Yates may be responsible for this mechanism [10].

Individual gel beads swollen in toluene were also subjected to uniaxial compression measurements. However, the interpretation of the compression test data of spherical gel particles is complicated due to the significant variation of the contact area between the wall and the originally spherical gel during deformation. For a sphere with a constant volume during deformation, Hertz derived the following equation for small deformation ranges [26–30].

$$F = \frac{4}{3}GD^{0.5}\Delta D^{1.5} \quad (4)$$

where  $F$  is the force,  $G$  is the elastic modulus, and  $\Delta D$  is the deformation,  $\Delta D = D - D'$ ,  $D$  and  $D'$  are the initial (swollen) undeformed and deformed diameters of gel sample, respectively. The Hertz theory (Eq. (4)) considers the contact deformation of elastic spheres under normal loads in the absence of adhesion and friction.

Fig. 5A shows force  $F$  versus deformation  $\Delta D$  plots of a series of swollen PIB beads of various diameters  $D$ , prepared by technique A. The force  $F$  is a non-linear function of the resulting deformation. According to Eq. (4),  $(3/4)F/D^{0.5}$  vs  $\Delta D^{1.5}$  plots should be linear for a given bead, with a slope equals to its elastic modulus. Indeed, linear plots were obtained for all the beads studied in the range of deformation ratios above 5%. In Fig. 5B,  $(3/4)F/D^{0.5}$  is plotted against  $\Delta D^{1.5}$  for swollen beads formed at 20 v/w%  $S_2Cl_2$

using both techniques and for the conventional beads. It is seen that the slopes of the regression lines corresponding to the elastic moduli  $G$  of the hydrogels vary depending on the bead diameter. However, no correlation was found between the diameter  $D$  and the elastic modulus  $G$  of the gel beads. The variations in the stress–strain curves shown in Fig. 5B depending on the bead diameter were in the range of experimental error. The average values of the modulus of the beads collected in the last column of Table 1 show that the moduli of the porous beads with 20%  $S_2Cl_2$  formed by the techniques A and B are 1.4 and 3.6 kPa, respectively, much larger than the modulus of conventional beads, which is about 0.3 kPa. Thus, crosslinking at ambient temperature produces very soft gels probably due to the hydrolysis of part of the crosslinker molecules. However, since the droplets are in a frozen state by techniques A and B, hydrolysis is prevented during the reactions leading to a larger number of crosslinks between the polymer chains. Table 1 also shows that decreasing crosslinker content also decreases the elastic modulus of porous beads. Further, the beads prepared by technique A exhibit larger swelling ratios and smaller moduli of elasticity than those formed by technique B. This is a result of the precooling step in liquid nitrogen which slows down the crosslinking reactions.

Fig. 6A compares the response rates of PIB beads prepared by three different techniques at 20% crosslinker. Here, the normalized gel volume  $V_{rel}$  (volume of the gel bead at time  $t$ /equilibrium swollen volume in toluene) is plotted against the time  $t$  of deswelling in methanol and re-swelling in toluene. The measurements were carried out by on-line monitoring of the diameter of the gel beads immersed into the solvent under an optical microscope coupled with an automatic image analyzing system. Porous gel beads attain their equilibrium collapsed and swollen states within 10 min. Although the conventional gel bead formed at 20 °C also deswells in methanol relatively rapid within 15 min, its re-swelling in toluene to attain the equilibrium swollen state requires about half day. The fast responsivity of the gel beads formed at –18 °C is

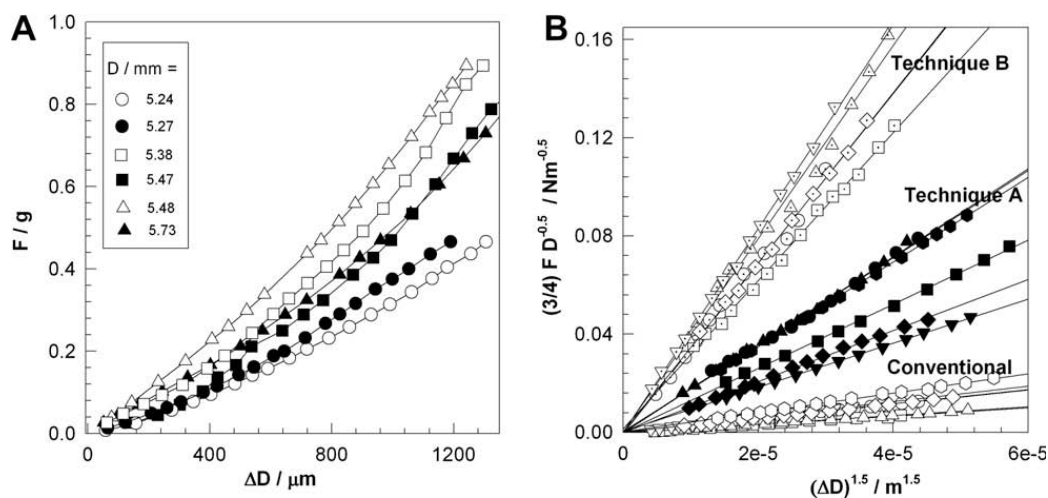
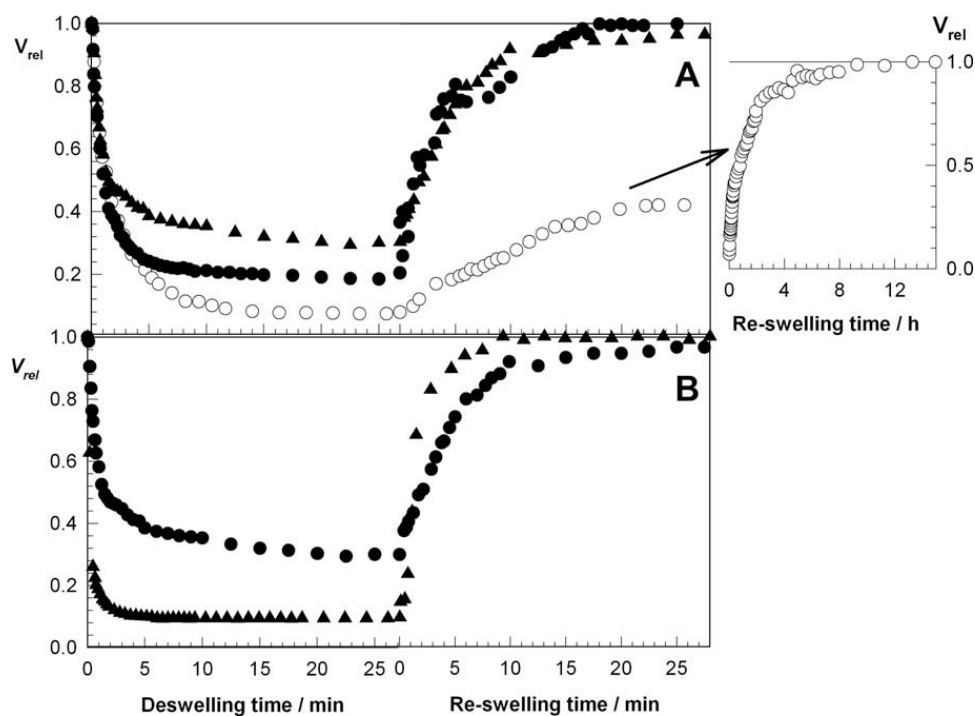


Fig. 5. (A) Force  $F$  versus deformation  $\Delta D$  plots of a series of beads obtained by technique A of various swollen diameters  $D$  in toluene, as indicated in the figure.  $S_2Cl_2 = 20$  v/w%. PIB concentration = 10 w/v%. (B) Stress–strain data of PIB gel beads of various diameters formed at 20 v/w%  $S_2Cl_2$  concentration.



**Fig. 6.** The normalized volume  $V_{rel}$  of PIB gel beads shown as a function of the time of deswelling in methanol and re-swelling in toluene. (A) PIB beads prepared by techniques A (●), B (▲), and conventional beads (○).  $S_2Cl_2 = 20$  v/w%. (B) PIB beads prepared by techniques B at 5 (▲) and 20 v/w%  $S_2Cl_2$  (●). PIB concentration = 10 w/v%.

due to their large pore volumes as well as the hole inside the beads which provide easy penetration of the solvent molecules within the network structure. Fig. 6B illustrates the response rate of macroporous particles formed at various concentrations of  $S_2Cl_2$ . It is seen that both swelling and deswelling rates were further improved by decreasing the crosslinker concentration in the reaction solution.

The gel beads prepared at  $-18$  °C by techniques A or B exhibited not only a high modulus of elasticity (Table 1); they were also very tough and can be compressed up to about 100% strain without any crack development. This is illustrated in Fig. 7 showing the compression of a swollen gel bead prepared by technique B using tweezers. As the gel bead is squeezed, it releases almost all its solvent so that it can completely be compressed (images A–C). After the release of the load and, after addition of toluene, the bead recovers its original shape and volume within 30 s (images D–E). In contrast, however, compression of the gel beads prepared at  $20$  °C resulted in their irreversible deformation and the spherical shape of the particles is disrupted even in the presence of toluene.

The high degree of toughness of the low temperature gel beads suggests that they can be used in separation processes in which the separated compounds can easily be recovered by compression of the beads under a piston. For example, the reusability of the sorbents and the recoverability of the pollutants are important aspects in oil spill cleanup procedures for the removal of crude oil and petroleum derivatives from surface waters [31]. To test the recoverability of the solvents from the beads and the reusability of the particles, individual swollen porous PIB particles were compressed under a force of  $14 \pm 3$  N. Under this condition, the particles formed at  $-18$  °C could be completely compressed. The solvent recoverability was determined by subjecting the particles to successive sorption–squeezing cycles to toluene as well as crude oil under identical conditions. For this purpose, each PIB bead was first immersed into 20 ml of toluene or crude oil for 1 min and then, it was left to drip for 30 s. The swollen bead was weighed and squeezed for 30 s under a force of  $14 \pm 3$  N. Then, it was weighed again to calculate the amount of toluene or crude oil sorbed by 1 g of dry bead. This sorption–squeezing cycle was repeated 30 times to



**Fig. 7.** Photographs of a swollen PIB gel bead formed at  $-18$  °C by technique B during complete compression (A–C). After compression, addition of toluene converts the gel bead back to its initial state (D and E).  $S_2Cl_2 = 20\%$ . PIB concentration = 10 w/v%. The scaling bar (for all images) is 2 mm.

obtain the recycling efficiency and continuous extraction capacity of the porous particles.

The results are shown in Fig. 8A where the uptake capacity of the particles in each cycle for toluene (filled symbols) and crude oil (open symbols) is plotted against the number of sorption–squeezing cycles. The particles were prepared by techniques A (circles) and B (triangles) at a crosslinker concentration of 20%. The results clearly demonstrate that the amount of toluene or crude oil separated from the liquid phase is constant in each cycle, i.e.,  $20.6 \pm 0.5$  g/g and  $18.2 \pm 0.3$  g/g for the particles formed by technique A in contact with toluene and crude oil, respectively. Further, comparing with the maximum toluene uptake capacity of the particles ( $q_w - 1$ , dotted lines in Fig. 8A), the particles extract toluene with a capacity only about 20% below its maximum capacity, indicating high continuous extraction capacity of the rubber particles. It must be noted that the particles could totally be compressed in each cycle without any damage or any change in their spherical shape. From the

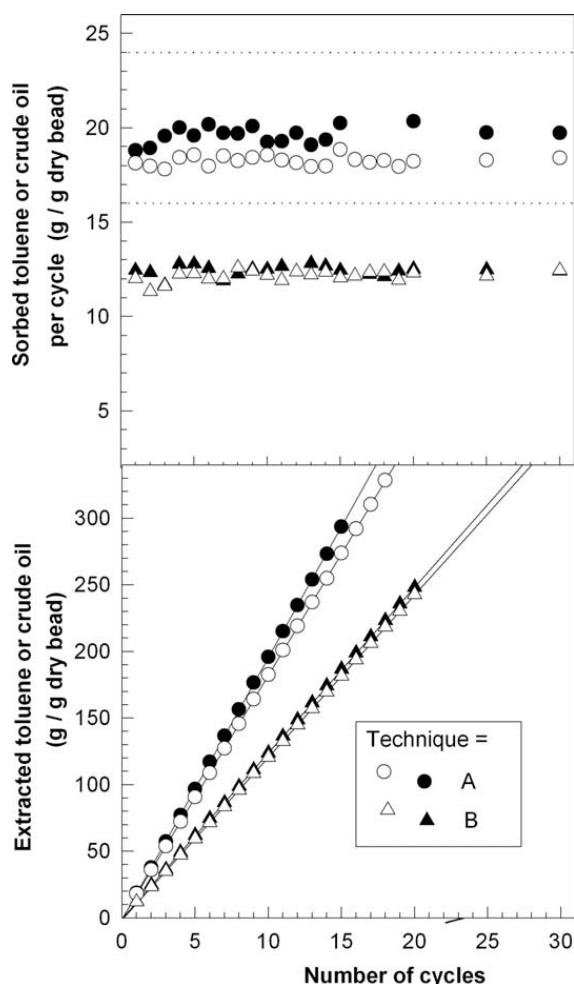


**Fig. 8.** Continuous extraction capacities of the particles prepared by techniques A (circles) and B (triangles) for toluene (filled symbols) and crude oil (open symbols).  $S_2Cl_2 = 20$  v/w%. PIB concentration = 10 w/v%. (A) The amount of toluene or crude oil separated in each cycle shown as a function of the number of cycles. The dotted lines represent the maximum toluene uptake capacities ( $q_w - 1$ ) of the particles. (B) The total amount of toluene or crude oil separated by the particles shown as a function of the number of cycles.

data in Fig. 8A, the total mass of toluene or crude oil separated from the bulk liquid phase can be calculated by summing up the uptake capacities of the particles in each cycle. Fig. 8B shows these results where the amount of separated toluene or crude oil is plotted against the cycle number. 365 g of crude oil can be separated from the liquid phase by use of 1 g of particles formed by technique A within 20 sorption–squeezing cycles. Experiments were also conducted using test solutions of 280 ml in volume with a crude oil layer of approximately 1 cm thickness on the water surface [32]. Macroporous PIB particles sorbed crude oil, but not water, with the same capacity as given in Fig. 8A. Further, the beads remained on the water surface both before and after the sorption process.

#### 4. Conclusion

Macroporous millimeter-sized organogel particles containing a single large hole in their surfaces were prepared by solution crosslinking of PIB in benzene using  $S_2Cl_2$  as a crosslinker at  $-18$  °C. The particles display a two phase morphology indicating that both cryogelation and reaction-induced phase separation mechanisms are operative during the formation of the porous structures. The beads exhibit moduli of elasticity of 1–4 kPa, much larger than the moduli of conventional nonporous organogel beads formed at 20 °C. The gel particles also exhibit fast responsiveness against the external stimulus (solvent change) due to their large pore volumes (4–7 ml/g). The gel particles are very tough and can be compressed up to about 100% strain during which almost all the solvent content of the particles is released without any crack development. The sorption–squeezing cycles of the beads conducted 30 times show that they can be used in oil spill cleanup processes in which the separated crude oil can easily be recovered by compression of the beads under a piston.

#### Acknowledgements

Work was supported by the Scientific and Technical Research Council of Turkey (TUBITAK), TBAG –107Y178. The author O. O. thanks Turkish Academy of Sciences (TUBA) for financial support.

#### References

- [1] Bergbreiter DE. Self-assembled, sub-micrometer diameter semipermeable capsules. *Angew Chem Int Edn Eng* 1999;38:2870–2.
- [2] Schacht S, Huo Q, Voigt-Martin IG, Stucky GD, Schuth F. Oil-water interface templating of mesoporous macroscale structures. *Science* 1996;273:768–71.
- [3] Cohen I, Li H, Houghland JL, Mrksich M, Nagel SR. Using selective withdrawal to coat micro particles. *Science* 2001;292:265–7.
- [4] Caruso F. Nanoengineering of particle surfaces. *Adv Mater* 2001;13:11–22.
- [5] Loscertales IG, Barrero A, Guerrero I, Cortijo R, Marquez M, Gnanou AM. Micro/nano encapsulation via electrified coaxial liquid jets. *Science* 2002;295:1695–8.
- [6] Wong MS, Cha JN, Choi KS, Deming TJ, Stucky GD. Assembly of nanoparticles into hollow spheres using block copolypeptides. *Nano Lett* 2002;2:583–7.
- [7] Huang H, Remsen EE, Kowalewski T, Wooley KL. Nanocages derived from shell cross-linked micelle templates. *J Am Chem Soc* 1999;121:3805–6.

- [8] Croll LM, Stöver HDH. Formation of tectocapsules by assembly and cross-linking of poly(divinylbenzene-*alt*-maleic anhydride) spheres at the oil–water interface. *Langmuir* 2003;19:5918–22.
- [9] Im SH, Jeong U, Xia Y. Polymer hollow particles with controllable holes in their surfaces. *Nature* 2005;4:671–5.
- [10] Yin W, Yates MZ. Effect of interfacial free energy on the formation of polymer microcapsules by emulsification/freeze-drying. *Langmuir* 2008;24:701–8.
- [11] Velev OD, Furusawa K, Nagayama K. Assembly of latex particles by using emulsion droplets as templates. 1. Microstructured hollow spheres. *Langmuir* 1996;12:2374–84.
- [12] Guan G, Zhang Z, Wang Z, Liu B, Gao D, Xie C. Single-hole hollow polymer microspheres toward specific high-capacity uptake of target species. *Adv Mater* 2007;19:2370–4.
- [13] He X, Ge X, Liu H, Wang M, Zhang Z. Cagelike polymer microspheres with hollow core/porous shell structures. *J Polym Sci A: Polym Chem* 2007;45:933–41.
- [14] Ceylan D, Okay O. Macroporous polyisobutylene gels: A novel tough organogel with superfast responsivity. *Macromolecules* 2007;40:8742–9.
- [15] Dogu S, Okay O. Tough organogels based on polyisobutylene with aligned porous structures. *Polymer* 2008;49:4626–34.
- [16] Lozinsky VI, Vainerman ES, Korotaeva GF, Rogozhin SV. Study of cryostructurization of polymer systems. *Colloid Polymer Sci* 1984;262:617–22.
- [17] Lozinsky VI. Cryogels on the basis of natural and synthetic polymers: Preparation, properties and applications. *Russ Chem Rev* 2002;71:489–511.
- [18] Gundogan N, Melekaslan D, Okay O. Rubber elasticity of poly(*N*-isopropylacrylamide) gels at various charge densities. *Macromolecules* 2002;35:5616–22.
- [19] Sayil C, Okay O. Macroporous poly(*N*-isopropyl) acrylamide networks: Formation conditions. *Polymer* 2001;42:7639–52.
- [20] Melekaslan D, Gundogan N, Okay O. Elasticity of poly(acrylamide) gel beads. *Polymer Bull* 2003;50:287–94.
- [21] Okay O, Durmaz S, Erman B. Solution crosslinked poly(isobutylene) gels: synthesis and swelling behavior. *Macromolecules* 2000;33:4822–7.
- [22] Okay O. Macroporous copolymer networks. *Prog Polymer Sci* 2000;25:711–79.
- [23] Krigbaum WR, Flory PJ. Statistical mechanics of dilute polymer solutions. V. Evaluation of thermodynamic interaction parameters from dilute solution measurements. *J Am Chem Soc* 1953;75:5254–9.
- [24] Erman B, Flory PJ. Critical phenomena and transitions in swollen polymer networks and in linear macromolecules. *Macromolecules* 1986;19:2342–53.
- [25] Eichinger BE, Flory PJ. Thermodynamics of polymer solutions. Part 2. Polyisobutylene and benzene. *Trans Faraday Soc* 1968;64:2053–60.
- [26] Hertz H. Über die Berührung Fester Elastischer Körper (on the Contact of Elastic Solids). *J Reine und Angewandte Mathematik* 1881;92:156. In: Jones DE, Schott GA, editors. *Miscellaneous papers* b H. Hertz. London: Macmillan; 1896.
- [27] Knaebel A, Rebre SR, Lequeux F. Determination of the elastic modulus of superabsorbent gel beads. *Polymer Gels Netw* 1997;5:107–21.
- [28] Briscoe BJ, Liu KK, Williams DR. Adhesive contact deformation of a single microelastomeric sphere. *J Colloid Interface Sci* 1998;200:256–64.
- [29] Barquins M, Shanahan MER. Effect of surface cavities on static and dynamic adhesion to an elastomer. *Int J Adhes Adhes* 1997;17:313–7.
- [30] Lu WM, Tung KL, Hung SM, Shiau JS, Hwang KJ. Compression of deformable gel particles. *Powder Technol* 2001;116:1–12.
- [31] Adebajo MO, Frost RL, Kloprogge JT, Carmody O, Kokot S. Porous materials for oil spill cleanup: A review of synthesis and absorbing properties. *J Porous Mat* 2003;10:159–70.
- [32] Ceylan D, Dogu S, Karacik B, Yakan SD, Okay OS, Okay O. Evaluation of butyl rubber as sorbent material for the removal of oil and polycyclic aromatic hydrocarbons from seawater. *Environ Sci Technol*, doi:10.1021/es900166v.